Bishop Moore College

Mavelikara

Project Report On

Synthesis and Characterization of Pure and Cobalt Doped Magnesium Oxide Nanoparticles

Dissertation submitted to the University of Kerala

in partial fulfilment of the requirement for the award of the Degree of

Bachelor of Science in Physics

By

Anjitha J Kumar Reg No: 23019101004

Blessy A B Reg No: 23019101026

Vishnu Priya A Reg No: 23019101014

Under the guidance of

MERIN GEORGE

ASSISTANT PROFESSOR, DEPARTMENT OF PHYSICS

BISHOP MOORE COLLEGE MAVELIKARA

CERTIFICATE

This is to certify that the dissertation entitled “Synthesis and Characterization of Pure and Cobalt doped Magnesium Oxide Nanoparticles” by Anjitha J Kumar(Reg. No: 23019101004), Blessy A B(Reg No: 23019101026) & Vishnu Priya A(Reg No: 23019101014) for the award of the degree of Bachelor of Science in Physics is an authentic work under my supervision and guidance during the period from 2019–2022.

Also certified, that the dissertation represents a team work from the part of the candidates.

Merin George

Assistant Professor

Department of Physics

Bishop Moore College, Mavelikara

Examiners:

1.

2.

DECLARATION OF ORIGINALITY

We, Anjitha J Kumar(Reg. No:23019101004) Blessy A B(Reg No: 23019101026) & Vishnu Priya A(Reg No: 23019101014) hereby declare that this dissertation entitled “Synthesis and Characterization of Pure and Cobalt doped Magnesium Oxide Nanoparticles” represents my original work carried out as a Bachelor of Science students of University of Kerala and to the best of our knowledge, it contains no material previously published or written by another person, nor any material presented for the award of other degree or diploma of University of Kerala or any other institution. Any contribution made to this research by others, with whom we have worked at University of Kerala or elsewhere, is explicitly acknowledged in the dissertation. Work of other authors cited in this dissertation have been duly acknowledge under the section “Reference”. We are fully aware that in case of non-compliance detected in future, the Senate of University of Kerala may withdraw the degree awarded to us on the basis of the present dissertation.

Anjitha J Kumar

Blessy A B

Vishnu Priya A

ACKNOWLEDGEMENT

Foremost, we would like to express my sincere gratitude to our guide Merin George, Assistant Professor, Bishop Moore College, Mavelikara for her continuous support, patience, motivation, enthusiasm and most knowledge. She was always a source of inspiration to us. Her guidance helped in all the time of research and writing this project. We could not imagine having a better advisor and mentor for our research. The work could not have been possible without her worthy suggestions and constant co-operation.

Besides our advisor, we also thankful to Dr D Sajan, Head of the department& Assistant professor, Bishop Moore College, Mavelikara for the help and guidance he provided to us for the initiation of this project. His Dynamism, vision, sincerity and motivation have deeply inspired us. Our heart is fulfilled with deep sense of thankfulness and obeisance to our teachers for their valuable suggestions. We also express our thanks to all faculty members of Bishop Moore College, Mavelikara for their constant support.

Our sincere thanks and gratitude to Ayona K Jose for her kind support during the project work. We are grateful for her inspiring and valuable suggestions during the entire period of our project work, which enabled us to complete the work successfully.

We are grateful to our parents for their love, prayers, caring and sacrifices. We also thank our friends for giving us strength.

Anjitha J Kumar

Blessy A B

Vishnu Priya A

CONTENTS

ABSTRACT

This project work covers the synthesis as well as structural and optical characterization of pristine and cobalt doped MgO nanoparticles. Nanostructures of pure and Co doped MgO have been synthesized using a modified auto-combustion method. The good crystallinity as well as crystalline size of 21.04nm and 23.56nm for pure and doped samples respectively have been manifested from XRD analysis. An enhancement of the crystalline quality of the nanoparticles and hence a decrease in grain boundary scattering is indicated by an increase in crystalline size with the increase in Co concentration. A general trend of absorption and a decrease in absorbance with increase in the wavelength of incident radiation have been brought out from UV-Visible spectra. Optical bandgaps of 2.75eV and 2.47eV respectively for MgO nanoparticles and Co doped MgO nanoparticles have been revealed from Tauc plot analysis.

CHAPTER 1

INTRODUCTION

1.1 Nanotechnology

Nanomaterials represents a significant aspect of nanotechnology which deals with various studies involving particles ranging between 1 and 100 nm at least in one spatial dimension. Compared to their bulk counterpart and molecular components, nanomaterials show unique electronic, optical and mechanic properties. Nanotechnology has a high impact on many fields including physics, engineering, biology, agriculture, food sciences and so on. The nanomaterials have a relatively larger surface area when compared to the same mass of material produced in a larger form. This makes the nanomaterials more chemically reactive and affects their strength or electrical properties. At the nanoscale, a quantum effect dominates the behaviour of matter. Nanoparticles and nanostructured materials have gained prominence in technological advancements due to their tunable physicochemical characteristics such as melting point, electrical and thermal conductivity, catalytic activity, light absorption and scattering resulting in enhanced performance over their bulk counterparts [1].

Large scale productions of nanoscale materials are usually very difficult which has led to its synthesis and studies in lab scale conditions. The productions of innovative and enhanced materials are achieved by either top-down or bottom-up approaches which are the two approaches for the synthesis of nanomaterials. Top-down manufacturing involves starting with a larger piece of material and etching, milling or machining a nanostructure from it by removing material (as, for example, in circuits on microchips). This can be done by using techniques such as precision engineering and lithography and has been developed and refined by the semiconductor industry over the past 30 years. Typical top-down processes are attrition and milling. In the bottom-up approach, molecular components arrange themselves into more complex assemblies from the bottom. Large numbers of atoms, molecules or particles are used or created by chemical synthesis and then arranged through naturally occurring processes into a desired structure. An example for the bottom-up approach is the synthesis of nanoparticles by colloidal dispersion. This method generally produces nanostructures with defects fewer than that produced by the top-down approach. In hybrid approach, both these techniques are employed. The dimensions controlled by both approaches are of a similar order and this leads to exciting new hybrid methods of manufacture [2].

The ideas and concepts behind nanotechnology started with the lecture entitled “There is plenty of room at the bottom” by physicist Richard Feynman. In the 1980s, two major

breakthroughs initiated the growth of nanotechnology. First was the invention of scanning tunnelling microscope which provided unprecedented visualization of individual atoms and bonds. Second, the discovery of fullerenes by Harry Kroto, Richard Smalley and Robert Curl. In its original sense, nanotechnology refers to the projected ability to construct items from the bottom up, using advanced techniques and tools to make complete and high-performance products.

Nanotechnology enables to manufacture lighter, stronger and programmable materials that require less waste than with conventional manufacturing and promises greater fuel efficiency in land transportation, ship, aircraft and space vehicles. The photoelectric materials enable the manufacture of cost-efficient solar-energy panels and semiconductor devices. Apart from a lot of new and futuristic applications, some well-known products such as paints and processes that use chemical catalysis like petroleum and other chemical processing rely on the properties of nanoparticles [3]

Significant challenges are to be overcome for the realization of the benefits of nanotechnology. New and sophisticated tools are needed to control the properties and structure of materials at the nanoscale. Significant improvements in computer simulations of atomic and molecular structures are essential for the understanding of the same. Today's scientists and engineers are exploring a wide variety of ways to deliberately make materials at the nanoscale to take advantage of their enhanced properties such as higher strength, increased control of light spectrum and greater chemical reactivity than their bulk counterpart [4].

1.1.1 Nanomaterial

Later part of the twentieth century witnessed a spectacular turn in the way we understood material science. Nanoscale materials are defined as a set of substances where at least one-dimensions in the nanometer range. A nanometer is one millionth of a millimeter. The smallest nano length is similar to the size of ten hydrogen atoms. [5] With the finding that material characteristics could also be changed by changing the size, keeping the chemical composition intact changed the approach toward the field.

The drastic characteristic change of materials is generally explained using few basic ideas.

- Quantum Confinement
- Surface volume ratio

Quantum Confinement: The methodology of varying the material characteristics with size was feasible only in a specific size regime, called the quantum confinement regime and the variation in a specific material characteristic invariably affected the other characteristics of the same

material as well. As we know that the genesis of most material properties such as optical, magnetic, mechanical and chemical lies in the states of electrons in the constituting atoms, their configuration in the atomic structures and the way these bonds with the neighboring atoms in a molecular system. [6]

These electrons experience 'confinement effects' when those are trapped in a nanometer sized structure of the material. It is the 'confinement effects' that makes the material characteristics unusual and generally size dependent. Our current understanding on the wave nature of the microphysical particles such as electrons and the quantum mechanics provide a fundamental basis for explaining the 'confinement effects'. Since the typical de Broglie wavelength of electrons is in the range on nanometers, the 'confinement effects' are pronounced and observable when the confining system is of the comparable size. Nanostructure shows size dependent properties different from those of a macroscopic semiconductor if one or more dimensions of the structure are comparable to wavelength of light or wavelength of electrons and holes. The quantum effects arise in systems, which confine electrons to regions comparable to their de Broglie wavelength. In other words, if the physical size of a material structure becomes smaller, the quantum mechanical effects become observable. Surface volume ratio: Another equally important thing is the ratio of surface area to the volume of a material structure, which tends to increase when the particle size is decreased. In macro scale, volume dependent properties are dominant but in nano scale the surface area dependent material properties start dominating or anomalous behaviors are observed in the Nano-scale regime. For example, Nano-particle catalysts are found to be chemically more effective than the bulk catalysts. Similarly, electric field related effects are also enhanced in the Nano- particles due to their sheer small size. For example, metal nanoparticle X-ray targets have been found to produce harder X-rays with enhanced yields.

1.2 Classification Of Nanomaterials

Nanomaterials, with their constituent phase or grain structures modulated on a length scale less than 100 nm are now artificially synthesized by a wide variety of physical, chemical and mechanical methods.[6] Nanostructured materials with modulation dimensionalities of zero, one, two and three are considered. The basic principles involved in the synthesis of these new materials are discussed in terms of the various special properties sought using selected examples from particular synthesis and processing methodologies. The classification of nanomaterials (NMs) mainly depends on the morphology, dimensionality, size, and agglomeration state and

composition structure. They are classified into two major groups as consolidated materials and nanodispersions. NMs are several types, like organic-based, inorganic-based, as well as composite-based NMs. Carbon-based NMs are a distinct class of nanomaterials, which are made up of carbon atoms, among which are fullerene, graphene, nanodiamonds, and carbon nanotubes (CNTs). The one-dimensional nano dispersive systems are termed as nanopowders and nanoparticles. The nanoparticles are further classified as nanocrystals, nanoclusters, nanotubes, etc. Nanomaterials are often classified depending upon the number of their dimensions falls under nanoscale.

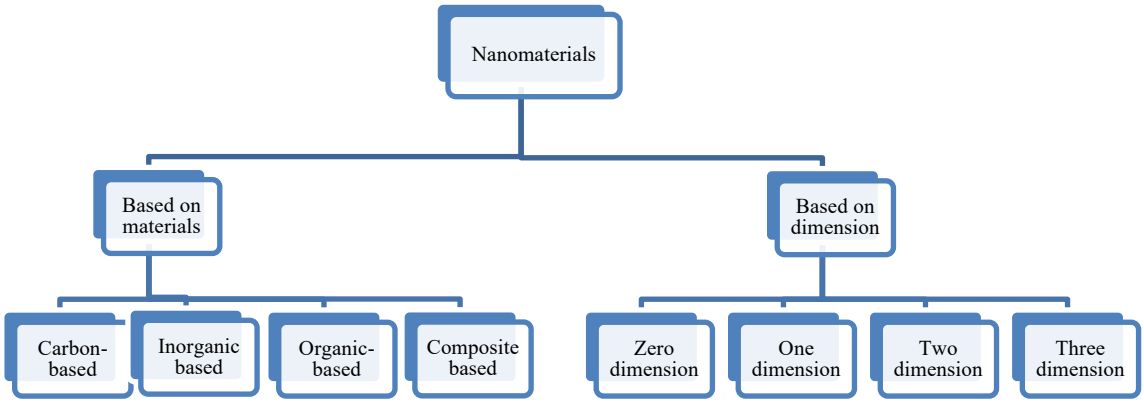

Figure1.1 Classification of nanomaterials based on materials and dimension

1.2.1 Zero-dimensional Nanomaterials

These are the materials whose all dimensions are measured within the nanoscale. The most common representation of zero-dimensional nanomaterials is nanoparticles. In zero dimensional nanoparticles, the movements of electrons are confined in all three dimensions. Some examples are graphene quantum dots, carbon quantum dots, and magnetic nanoparticles and so on. Due to ultra-small size, quantum confinement effect, excellent physical and chemical properties, zero dimensional nanomaterials have great potential in ion detection, biomolecular recognition, disease diagnosis and detection of pathogens. They also have an excellent affinity with biomolecules and thus providing the possibility for the development of biosensor platforms [7].

1.2.2 One-dimensional Nanomaterials

One-dimensional materials are in nanoscale in two dimensions. Examples include nanotubes, nano-fibers, nanowires, nanorods and nano-filaments. Electrons are confined within two dimensions, indicating that electrons cannot move freely. They are amorphous or crystalline, metallic, ceramic or polymeric similar to the zero-dimensional materials. One-dimensional nanostructures with a high aspect ratio such as nanotubes and nanowires are considered to be

ideal field emitters that emit electrons in a low electric field. Recently, one dimensional nanostructure such as wires, rods, belts and tubes have become the focus of intensive research owing to their unique applications in microscopic physics and fabrication of nanoscale devices. One dimensional nanostructure provides a better system to investigate the dependence of electrical and mechanical properties on dimensionality and quantum confinement. One dimensional nanomaterial plays an important role as both interconnects and
Functional units in fabricating electronic, optoelectronic, electrochemical and electromechanical devices with nanoscale dimensions [8].

1.2.3 Two-dimensional Nanomaterials

These are ultra-thin nanomatertials with a high degree of anisotropy and chemical functionality. The majority of researches on 2D nanomaterials focus on its biomedical applications. Owing to their uniform shapes, high surface to volume ratios and surface charge, 2D nanoparticles such as carbon-based 2D materials, silicate clays and transition metal oxides provides enhanced physical, chemical and biological functionality. Important applications include drug delivery, imaging, tissue engineering and biosensors

Two-dimensional nanostructures (or quantum wells) have been extensively studied by the semiconductor community because they are conveniently prepared using techniques such as molecular beam epitaxy (MBE). Due to their high anisotropy and chemical functions, two-dimensional nanomaterials have attracted increasing interest and attention from various scientific fields including functional electronics, catalysis, supercapacitors, batteries and energy materials. In the biomedical field, 2D nanomaterials have made significant contributions to the field of nano-medicine, especially in drug delivery systems, multimodal imaging, bio-sensing, antimicrobial agents and tissue engineering .2D nanomaterials such as graphene oxide, silicate clays, double hydroxides, transition metal chalcogenides, boron nanosheets and tin telluride nanosheets possess excellent physical, chemical, optical and biological properties due to their uniform shapes, high surface to volume ratios and surface charge[9].

1.2.4 Three-dimensional Nanomaterials

Three-dimensional nanomaterials or bulk nanomaterials are materials that are not confined to the nanoscale in any dimension. These materials are characterized by having three arbitrarily dimensions above 100 nm. They can contain dispersions of nanoparticles, bundles of nanowires, nanotubes as well as multinanolayers. These are not confined to the nanoscale in any dimension.

Due to their high specific surface area, interconnected porous structure, light weight and high mechanical strength, carbon nano-fibre (CNF) based three dimensional nanomaterials have attracted much attention in many fields, especially in energy production/storage and

environmental science. 3D CNF-based nanomaterials are synthesized by electro-spinning deposition, CVD, templated synthesis, and hydrothermal synthesis. In some cases, the formation of 3D nanomaterials involves complex processes that include two or more of these techniques. Electrospinning is a facile technique used to fabricate 3D Polymer Nano-fibre (PNF) based scaffolds. In this process, the thicknesses of the electro-spun nano-fibrous scaffolds are proportional to the spinning time. Hence, the easiest way to form a 3D structure is to extend the collection time to increase the film thickness.

In addition, the electric field shielding and debilitating effect place a limit on the thickness of the deposited PNFs. Hydrogels and aerogels are common 3D network structure gels formed by chemical and physical cross-linking. Therefore, they have potential applications in the fields of energy storage, environmental remediation, strain/pressure sensors, insulators etc. This material with its high-water absorption and high water-retention are widely used in environmental science, energy storage, sensors, thermal insulators, biomedicine etc. [10].

1.3 Properties Of Nanomaterials

1.3.1 Mechanical Properties

Mechanical properties refer to the mechanical characteristics of materials under different environments and various external loads. Nanomaterials have excellent mechanical properties due to the volume-surface and quantum effects [11]. The addition of certain nanoparticles in a particular concentration can improve compressive strength, bending strength and tensile strength of materials. When the size of a particle approaches nanoscale with the characteristic length scale close to or smaller than de Broglie wavelength of the charge carrier or the wavelength of light, the periodic boundary condition of the crystalline particle is destroyed. Due to this, a lot of physical properties of nanoparticles are quite different from bulk materials, yielding a variety of new applications. For example, nanoparticles adsorbed in matrix materials have been used as carriers for delivering drug molecules. The lubricating properties of nanoparticle materials are used in the machines. Grain size is one of the main factors affecting the mechanical properties of nanomaterials. The effects of grain size on the mechanical properties of nanomaterials are mainly reflected in the microstructure. Nanoparticles have a considerable size effect and high surface activity. Since the nanoparticles are extremely small, their addition can fill the matrix's pores, reduce porosity, increase relative density, and improve mechanical properties [12].

1.3.2 Optical Properties

Semiconductor and metallic nanomaterials possess interesting linear absorption, photoluminescence emission and nonlinear optical properties. Enhanced optical emissions as well as nonlinear optical properties are exhibited by small sized nanomaterials due to the quantum confinement effect.

Silver and gold nanostructures exhibit fascinating optical properties due to their strong optical absorption in the visible region as a result of the collective oscillation of conduction band electrons, called surface plasmons. Surface Enhanced Raman Scattering (SERS) offers high sensitivity and molecular specificity that are needed for sensing and imaging applications. The optical properties of nanomaterials are very interesting because of their nanoscale dimension and presence of surface plasmon resonance character.

However, these properties are strongly influenced by a number of factors such as size, shape, surface functionalization, doping and interactions with other materials etc. The size dependent optical property of them is due to change in the optical energy bandgap, which in turn influences the surface plasmon resonance of the nanomaterials.

The optical bandgap increases with the decrease in particle size, especially for the semiconductor nanomaterials. Thus, the colloidal gold or silver nanoparticles produce different colors for different sizes, especially in the range of 1-10 nm. Surface plasmon resonance is only observed if the particle size of the materials is less than the wavelength of the incident radiation. Thus, nanomaterials can produce surface plasmon resonance, but not the bulk materials. The intensity of such surface plasmon resonance is directly proportional to the number of excited electrons and the dielectric constant of the medium used [13].

1.3.3 Electrical Properties

In bulk materials, conduction electrons are delocalized and travel freely till they are scattered by photons, impurities, grain boundaries etc. In nanoscale conductors, due to quantum effect, continuous bands are replaced with discrete energy states. The mean free path for inelastic scattering becomes comparable to the size of the system. In semiconductor quantum confinement of both the electron and hole leads to an increase in the effective band gap of the material with decreasing crystallite size. These effects lead to altered conductivity in nanomaterials.

1.4 Synthesis Methods

Engineered nanomaterial are resources designed at the molecular (Nano meter) level to take advantage of their small size and novel properties which are generally not seen in their

conventional, bulk counterparts. Research in nanostructured materials is motivated by the belief that ability to control the building blocks or nanostructure of the materials can result in enhanced properties at the macroscale: increased hardness, ductility, magnetic coupling, catalytic enhancement, selective absorption, or higher efficiency electronic or optical behavior [14]. There exist a number of methods to synthesize the nanomaterials which are categorized in two techniques “top down” and “bottom up”. Methods like solid state route and ball milling comes in the category of top-down approach, while wet chemical routes like sol-gel, co-precipitation, etc. come in the category of bottom-up approach [15]. The top-down methods involve the division of a massive solid into smaller and smaller portions, successively reaching to nanometer size. This approach may involve milling or attrition The second, “bottom-up”, method of nanoparticle fabrication involves the condensation of atoms or molecular entities in a gas phase or in solution to form the material in the nanometer range. The latter approach is far more popular in the synthesis of nanoparticles owing to several advantages associated with it [16].

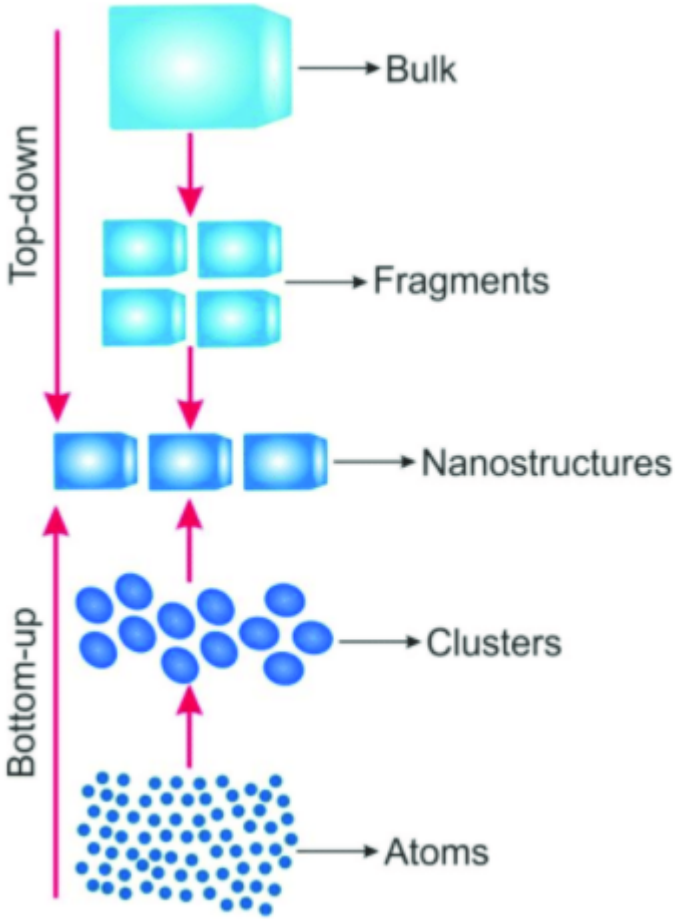

Figure 1.2: Schematic representation of top-down and bottom-up approaches for synthesis of nanomaterials.

There are many bottom-up methods of synthesizing metal oxide nanomaterials, such as hydrothermal, combustion synthesis, gas- phase methods, microwave synthesis and sol-gel processing. [17]. The top-down approach plays an important role in the synthesis and fabrication of nanomaterials. There are many methods of synthesis. A few are explained below.

1.4.1. Sol Gel Method

Sol-gel is a wet chemical based self-assembly process for nanomaterial formation. Sol-gel processing is a wet chemical route for the synthesis of colloidal dispersions of inorganic and organic-inorganic hybrid materials, particularly oxides and oxide-based hybrids. From such colloidal dispersions, powders, fibers, thin films and monoliths can be readily prepared. Typical sol-gel processing consists of hydrolysis and condensation of precursors. Precursors can be either metal alkoxides or inorganic and organic salts. [18]. The sol-gel process consists of the following steps:

i) Preparation of a homogeneous solution either by dissolution of metal organic precursors in an organic solvent that is miscible with water, or by dissolution of inorganic salts in water

ii) Conversion of the homogeneous solution into a sol by treatment with a suitable reagent (generally water with or without any acid/base)

iii) Aging

iv) Shaping

v) Thermal treatment/ sintering.

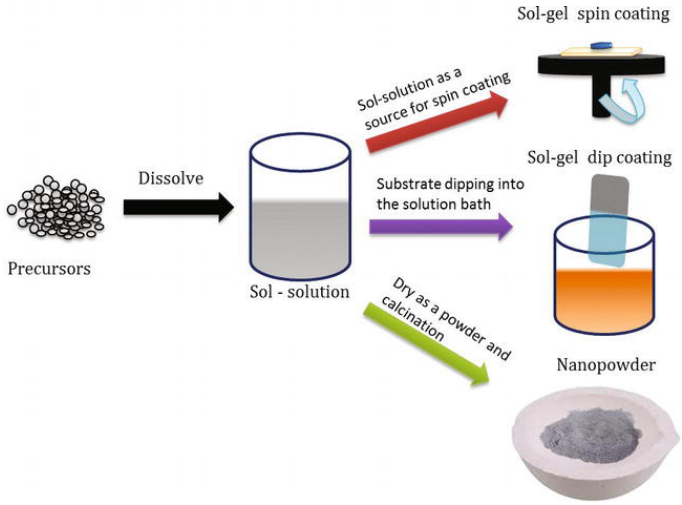

Figure.1.3 Sol-gel method

Sol–Gel method involves preparation of sol, successive gelation followed by removal of solvent. It is very useful and easy method to produce nanostructures wherein precursors are homogeneously mixed in solvent to form an integrated continuous network of liquid phase (gel) which are then heat treated to form nanoparticles, controlling its morphology, shape and size. Yang et al. synthesised NiO nanowire employing sol–gel method.

1.4.2 Combustion Method

Combustion is a complex sequence of chemical reactions between a fuel and an oxidant accompanied by the production of heat or both heat and light in the form of either a glow or flames. The combustion uses rapid thermal degradation of precursor chemical reaction with oxygen has been effectively used for the synthesis of variety of metal oxides in nanoscale. Based on the fuels and their combinations with the metal ions sources (commonly metal nitrates, acetates, hydroxides), combustion process has classified into the following.

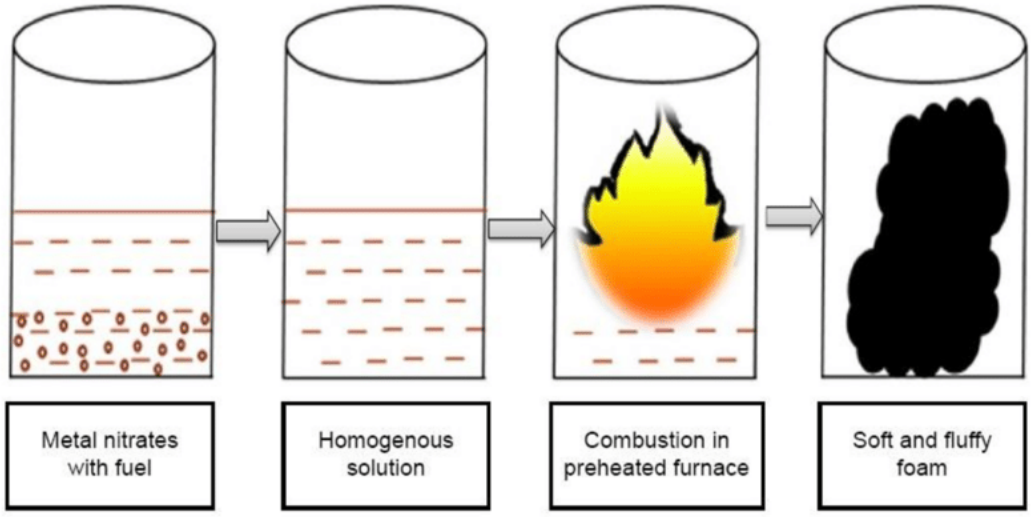

Figure 1.4. Combustion method

Combustion of Fuel: Oxidant Fuel-oxidant combustion technique involves an exothermic decomposition of a fuel– oxidant precursors such as urea- nitrate, glycinenitrate, DHF- nitrate, etc, relatively at lower temperatures. Also, it explores highly fast and self-sustaining exothermic reaction between the metal salts and organic fuels. The heat required for the phase formation is supplied by the reaction itself and not by an external source. During this ignition process, large volume of gases will evolve which prevent the agglomeration and lead to the formation of fine powders with nano structures. The release of heat during the combustion reaction depends on the fuel – oxidant stoichiometry in the precursor composition. The fuel – oxidant stoichiometry is used to calculate the required fuel, based on the thermo dynamical concepts used in the field of propellants and explosives, for the required nature of combustion process.

1.4.3 Co-precipitation

Co-precipitation is a facile and convenient approach to prepare magnetic nanoparticles. The technique consists of reducing a mixture of metallic ions (Fe^{3+} and Fe^{2+}) using a basic solution (usually NaOH or NH_3OH) at temperature below 100^0 C. The advantages of the co-precipitation method are the high yield, high product purity, the lack of necessity to use organic solvents, easily reproducible and low cost. However, the properties of the obtained particles such as size, shape, and composition are highly dependent on the reaction parameters like temperature, pH, ionic strength, kind of basic solution etc. Besides iron oxide nanoparticles obtained in this way are often not stable and hence are stabilized by using low molecular weight surfactants, or functionalized polymers. Homogenous precipitation is obtained via a process that involves separation of the nucleation and growth of the nuclei. The products are obtained as an insoluble species in supersaturation conditions. Typical co-precipitation synthetic methods involve the following stages (i) nanomaterials formation takes place from aqueous solutions or by reduction from aqueous solutions, electrochemical reduction and decomposition of metal-organic precursors with templates; (ii) metal chalcogenides are formed by the reactions of molecular precursors; (iii) microwave/sonication assists the co-precipitation to take place.

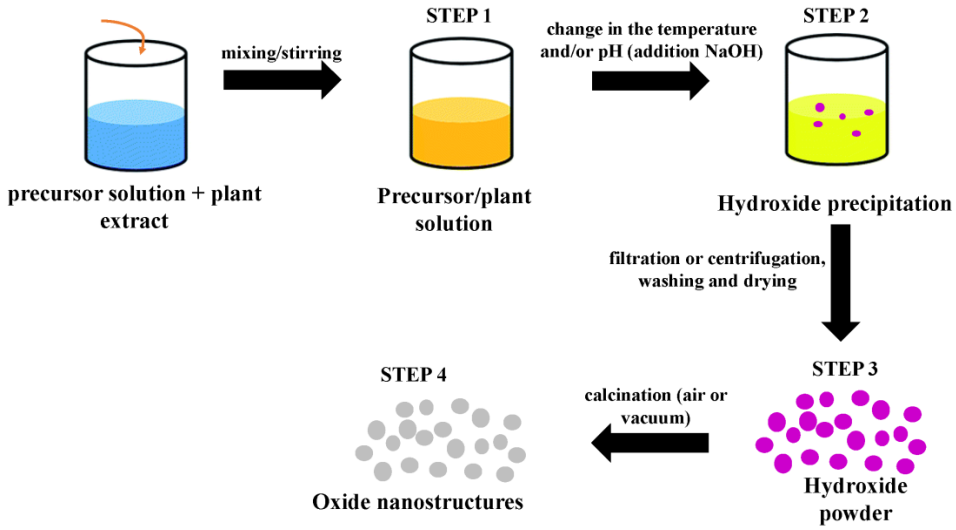

Figure 1.5. Co-precipitation method

In this method, the required metal cations from a common medium are co-precipitated usually as hydroxides, carbonates, oxalates, formates or citrates. These precipitates are subsequently calcined at appropriate temperature yield the final powder. For achieving high homogeneity, the solubility products of the precipitate of metal cations must be closer. Co-precipitation results in atomic scale mixing and hence the calcinating temperature required for the formation of final product is low.

1.4.4 Hydrothermal Method

Hydrothermal synthesis is one of the most commonly used methods for preparation of nanomaterials. It is basically a solution reaction-based approach. In hydrothermal synthesis, the formation of nanomaterials occurs in a wide temperature range from room temperature to very high temperatures. To control the morphology of the materials to be prepared, either low-pressure or high-pressure conditions can be used depending on the vapour pressure of the main composition in the reaction. Many types of nanomaterials have been successfully synthesised by the use of this approach.

Hydrothermal synthesis generates nanomaterials which are not stable at elevated temperatures. Nanomaterials with high vapour pressures can be produced by the hydrothermal method with minimum loss of materials. The compositions of nanomaterials to be synthesized can be well controlled in hydrothermal synthesis through liquid phase or multiphase chemical reactions [19]. The crystal growth is performed in an apparatus consisting of a steel pressure vessel called an autoclave, in which a nutrient is supplied along with water. A temperature gradient is maintained between the opposite ends of the growth chamber. The nutrient solute dissolves at the hotter end while it is deposited on a seed crystal at the cooler end which leads to the growth of the desired crystal. Advantages of the hydrothermal method over other types of crystal growth include the ability to create crystalline phases which are not stable at the melting point. Also, materials which have a higher vapour pressure near their melting points can be grown by the hydrothermal method. The method is also particularly useful for the growth of large good quality crystals while maintaining control over their composition. Disadvantages of the method include the need of expensive autoclaves and the impossibility of observing the crystal as it grows if a steel tube is used [20].

1.5 Magnesium Oxide

Nanostructured materials, and nanotechnology in general, have received considerable attention in the last few decades, with significant overlap in the techno-economic sector [21–23]. Nanomaterials can be further classified [24,25] based on (i) dimensionality (0D–3D), (ii) morphology (e.g., nanospheres, nanotubes, and nanowires), (iii) state (e.g., isometric, suspension, and agglomerates), or (iv) chemical composition (e.g., organic, inorganic, single component, and composites). The most important representatives of the single metal oxide group are silicon dioxide (SiO2), ferric oxide (Fe2O3), zinc oxide (ZnO), titanium dioxide (TiO2), and magnesium oxide (MgO) [26]. Due to their unique properties, these materials find applications in areas, such

as medicine, agriculture, information technology, electronics, energy, and environmental protection [27].

As mentioned earlier, one of the promising materials belonging to the single metal oxide group is magnesium oxide. Magnesium oxide, also referred to as periclase [28], is an inorganic material with a molar mass of 40.31 g/mol [29] and a density of 3.58 g/cm3 [30]. Its empirical formula is MgO, and its lattice consists of Mg2+ ions and O2− ions linked by an ionic bond in a 1s22s2p6 and 1s22s2p6 configuration, which means that the d-orbitals are empty in this case [31]. The magnesium oxide structure is of the rock-salt type (lattice parameter 4.21 Å [32] and cleaving on (100) and (111) planes. It is a wide band gap insulator. It has a cubic crystal structure with Fm-3m space group. In general, it consists of two intersecting Mg and O lattices that are offset relative to each other by 0.5 of the body diagonals. The electronic configuration and crystal structure are shown in Figure a.

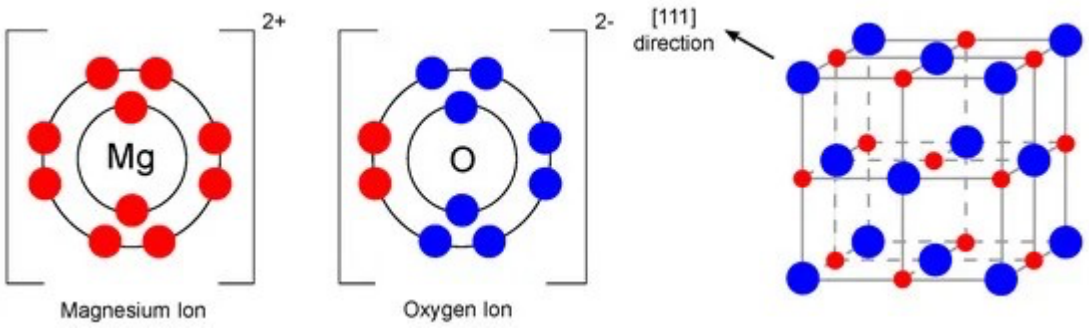

Figure a: Electronic configuration of Mg2+ and O2− ions and crystal structure of MgO (redrawn and adapted from [31,33]).

Magnesium oxide is produced by the calcination of magnesium carbonate or magnesium hydroxide. The latter is obtained by the treatment of magnesium chloride MgCl2 solutions, typically seawater, with limewater or milk of lime [34].

$$Mg2+ + Ca\,(OH)2 \rightarrow Mg\,(OH)2 + Ca2+$$

MgO is an attractive material which has many potential applications, such as water purification, optoelectronics, microelectronics, and additive in heavy fuel oil, paint, gas separation, bactericides, and insulator in industrial cables, crucibles, and refractory materials. Further, it has been used as an oxide barrier in spin tunneling devices as well as substrate in super conducting and ferroelectric film. The MgO nanoparticles have high catalytic activity. Due to high specific

surface area of nano-MgO materials, they are found to catalyze efficiently in variety of organic reactions [35–37]. MgO is a useful oxide that have been widely used for industrial applications such as in medicine, refractory materials, heating apparatus and infrared optics [38-40].

1.6 Literature Review

Mohammed. M. Obeid et al. [41], reported the synthesis of MgO nanoparticles by co-precipitation method. The synthesized samples were characterized using X-ray diffraction (XRD), differential thermal analysis (DTA) and UV-Visible (UV-Vis) spectroscopy. The UV–Visible absorption spectra showed a redshift with the increase in cobalt doping content in MgO host lattice while corresponding bandgap energy of cobalt doped MgO-NPs was decreased with the increase of doping concentration. The XRD patterns revealed the formation of rock salt MgO phase nanostructures. The coherent domain size increased from 7.44 nm to 8.11 nm with increasing Co doping amount up to x = 0.06. The microstructure of pure and doped MgO-NPs prepared by a simple co-precipitation method was studied by means of full pattern fitting technique. The optical properties were investigated by UV-Visible spectrometer. In addition, the effect of cobalt ions on the magnetic properties of the desired product was predicted based on Mulliken population analysis. The current analysis reveals that Co doped MgO nanoparticles are effective in improving various structural and optical properties.

Jingjun Wua et al. [42], reported the synthesis of Magnesium oxide (MgO) doped with cobalt (Co) semi-sintered pressure-transmitting medium (MCOPM) was prepared at 1200°C in air, starting with a pre-compressed mixture of MgO and cobalt oxide (CoO). The samples were characterized using powder X-ray diffraction, scanning electron microscopy, and thermal conductivity measurements. The results demonstrate that during the sintering process, the exchange of metal ions between the mixture powders introduced lattice defects into the MgO lattice structure, and an MgO–CoO solid solution was formed. Magnesium oxide (MgO) is widely used as a pressure-transmitting medium (PM) for high pressure and high-temperature (HPHT) experimentation. MgO with a doping level of 17 mol% Co turned out to be the most appropriate material for use as an HPHT pressure medium since higher doping led only a marginal increase in heat insulation. Moreover, the thermal conductivity of CoO doped MgO decreased with increasing CoO doping.

Balakrishnan et al. [43] synthesized MgO using the solution combustion method. They used magnesium nitrate as an oxidizer and urea as fuel. Using this method, they produced MgO with a cubic structure and crystallite size around 22 nm as seen from the XRD results. Through SEM analysis, the authors found that the particles are spherical and their size is uniform. Interestingly,

compared to other studies, the synthesized particles have a bandgap of only 2.9 eV. he as-prepared nanoparticles are analyzed using X-ray diffraction, FE-SEM, FTIR to study the microstructure. The sample is also analyzed using photoluminescence, and photocatalytic studies to investigate the optical and catalytic properties. FTIR analysis proved the presence of Mg-O bands. The degradation efficiency of 31, 66, 71 and 75 % is observed after 30-, 60-, 90- and 120-min irradiation. The photo catalytic studies revealed that the MgO nanoparticles, which degrade the MB dye effectively and MgO nanoparticles can be used as excellent adsorbents for degradation of effluents in the industries. MgO nanoparticles is used as a catalyst and its photocatalytic activity is analyzed using the photoreactor with UV light of 365 nm wavelength and 125 watts.

Suresh et al. [44] used an extract of Nephelium lappaceum L. And double distilled water for green synthesis, whereby magnesium nitrate was used as a precursor. They verified the cubic structure of MgO by the investigations that were carried out, and the average crystallite size was determined as 55 nm, which agreed very well with the SEM measurements (grain size 60–70 nm). The particle size of as-synthesized magnesium oxide powders measured by PSA was approximately 100 nm. The successful formation of magnesium oxide nanoparticles was confirmed employing XRD, SEM-EDX and PSA analysis. Biosynthesis of magnesium oxide nanoparticles was achieved by a novel, simple green chemistry procedure using Nephelium lappaceum L peel extract as a natural ligation agent. We have demonstrated the use of a natural, renewable and low-cost bio reducing agent such as Nephelium lappaceum L. peels effectively for the synthesis of magnesium oxide nanoparticles.

Devaraja et al. [45] described the properties of a nanocrystalline MgO powder that had been prepared from magnesium nitrate hexahydrate and sodium hydroxide by Solvothermal method. Their presented procedure resulted in porous magnesium oxide particles with an average crystallite size of 25 nm. Among the other reported properties of the synthesized particles was the optical energy bandgap (5.5 eV).

Wahab et al. [46] reported the synthesis of MgO nanoparticles using solgel method, who prepared MgO particles from magnesium nitrate together with sodium hydroxide. The procedures reported in this study led to the formation of the cubic form of MgO nanoparticles with a size of 50–60 nm. The chemical route, Sol-gel processes, has become a promising option for the synthesis and large-scale production of nanostructured materials as well as magnesium oxide. In this paper, we present synthesis and characterization of crystalline cubic shaped MgO nanoparticles by sol-gel method at room temperature. X-ray diffraction patterns indicate that the obtain nanoparticles are in good crystallinity, pure magnesium oxide periclase phase with

(200) orientation. Morphological investigation by FESEM reveals that the typical sizes of the grown nanoparticles are in the range of 50-70nm. This method is found to be a mild and efficient route for the large-scale industrial production of fine magnesium oxide nanoparticles without any template or expensive chemicals.

CHAPTER 2

SYNTHESIS & CHARACTERIZATION

2.2 Synthesis

Nanostructures of pristine and Co doped MgO are synthesized using a modified auto combustion method. A stoichiometric amount of Magnesium nitrate hexahydrate (merk, 98% purity) and citric acid (merk, 98% purity) are taken for the preparation of pristine MgO and Cobalt nitrate hexahydrate, citric acid, and Magnesium nitrate hexahydrate for Co doped MgO nanostructures. The mixture is dissolved in deionized water wherein citric acid is used as a fuel. 30 ml of nitric acid is added to the above solution. A solution with no precipitation and sedimentation is obtained after 30 minutes of stirring. Ammonia is added to maintain the pH as neutral. The solution is heated in a hot plate at about 250 ºC in the combustion chamber. On the completion of dehydration, internal combustion starts, and a black coloured powder is obtained. The resultant powder is heated to about 600 ºC for 3 hrs in the high-temperature furnace to remove impurities. The sintered samples are taken for different characterizations.

2.3 Characterization Methods

Characterization is a useful quantitative description of the constitution of the material. Basically, characterization is a description of the kinds of the location of the constituents, atoms and ions, to the extent that such a description is needed for correlation with properties, with performance, and for reproducing and improving the material. The characterisation tools used for this study are

1. X-Ray Diffraction (XRD)
2. UV- Visible Spectroscopy

2.3.1 X- Ray Diffraction (XRD)

X-Ray Diffraction (XRD) is the most commonly used technique in the determination of crystal structure of atoms.

X-ray diffractometer consist of three basic elements

i. An X-ray tube
ii. An X-ray detector
iii. A sample holds

X-rays are generated in a cathode ray tube by heating a filament to produce electrons, accelerating the electrons toward a target by applying a voltage, and bombarding the target material with electrons. When electrons have sufficient energy to dislodge inner shell electrons of the target material, characteristic X-ray spectra are produced. These spectra consist of several components, the most common being Kα and Kβ. Kα consists, in part, of Kα1 and Kα2. Kα1 has a slightly shorter wavelength and twice the intensity as Kα2. The specific wavelengths are characteristic of the target material (Cu, Fe, Mo, and Cr). Filtering by foils or crystal monochrometer is required to produce monochromatic X-rays needed for diffraction. Kα1 and Kα2 are sufficiently close in wavelength such that a weighted average of the two is used. Copper is the most common target material for single crystal diffraction, with CuKα radiation = 1.5418Å. These X-rays are collimated and directed onto the sample. As the sample and detector are rotated, the intensity of the reflected X-rays is recorded. When the geometry of the incident X-rays impinging the sample satisfies the Bragg Equation, constructive interference occurs and a peak in intensity occurs. A detector records and processes this X-ray signal and converts the signal to a count rate which is then output to a device such as a printer or computer monitor [47].

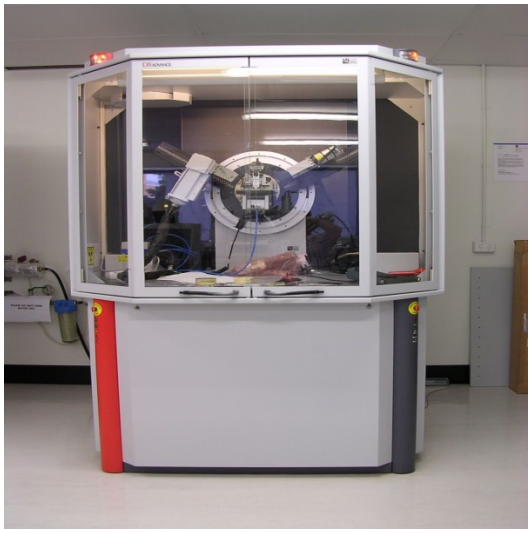

Figure 2.1: XRD Machine

The most commonly used X-ray instrument is the powder diffractometer. It has a scintillation or Geiger counter. The detector shows a range of scattering angles. Generally, it is a practice to mention scattering angle 2θ . The intensities are taken as peak heights. The d values can be calculated from the graph. A set of peaks and their heights is adequate for phase identification.

Bragg's law

In Bragg's law a crystal is viewed as a plane containing lattice points. The reflection of X-rays will take place from these planes with the angle of reflection is equal to angle of reflection as shown in the figure 2.5 below. From the figure BCD= BC+CD= d sinθ +d sinθ = 2d sinθ . The reflected beams are in phase when the path length between them is an integral multiple of the wavelength. This means the distance BCD = n λ. That is

$$n\lambda = 2d\sin\theta.$$

where n = 0,1,2,3…, d = interplanar spacing, λ = wavelength of incident X-rays, ɵ = Angle of reflection. This is the Bragg's law

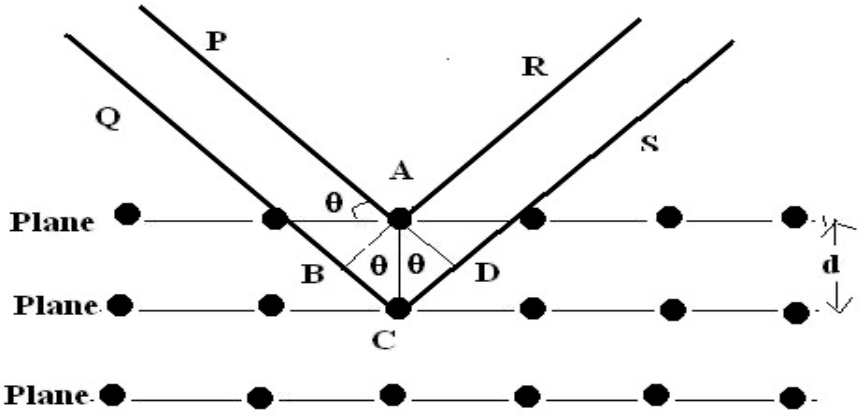

Figure: 2.2 Bragg's law analysis.

For crystal contain thousands of planes the Bragg's law imposes certain restrictions on angle of reflection. In that case diffraction peak will be broaden and the s effect is used to measure the size of particle by using Debye- Scherer formula

The average crystallite size is calculated from XRD pattern using Debye – Scherer formula,

$$\mathbf{D} = \frac{\mathbf{k} \times \boldsymbol{\lambda}}{\boldsymbol{\beta}\mathbf{cos}\boldsymbol{\theta}}$$

where λ is the wavelength of X -rays used (1.5406Å), k is the shape factor (0.89), β is the Full Width Half Maximum (FWHM) in radian and θ is the angle of diffraction

In the powder sample, there are a large number of crystallites (≈10^{12}per mm^3) oriented in all possible directions. When a monochromatic X-ray beam falls on the powder sample, all possible

combinations of θ and d are obtained, which satisfy Bragg's condition, and for any particular d, all orientations of the crystallites are obtained and, hence, the diffracted rays lie on the surface of a cone with the semi-vertical angle of 2θ, as shown in figure. If the sample has big grains, the diffraction ring or the arc will be spotty. To avoid it or make the arcs smooth, arrangement is made for the rotation of the sample on its axis.

2.3.2 Ultraviolet- Visible Spectroscopy

Ultraviolet –visible spectroscopy is the widely used technique to characterize organic and inorganic nanoparticles. UV-VISIBLE absorption spectroscopy used electromagnetic radiation between 200-800 nm .This radiation is divided between Ultraviolet (200-400nm) and Visible (400- 800 nm).This spectroscopy is also known as Electronic spectroscopy due to the absorption of UV radiation or Visible radiation by molecules lead to the transition between electronic energy levels of the molecules .The UV spectroscopy obeys Beer-Lambert law .The Beer Lambert law states that when a beam of monochromatic radiation is passed through solution of an absorbing substance the rate of decrease in intensity of radiation with the thickness of absorbing solution is proportional to the incident radiation as well as the concentration of the solution.

$$A = \log (I_0/I) = ECL$$

Where, A = Absorbance, I_0 = Intensity of light incident upon sample cell, I = Intensity of light leaving sample cell, C = molar concentration of solution, L = length of sample cell, E = molar absorptivity.

Molecules contain two types of electrons non – bonding electrons or π electrons which can absorb energy in the form of UV- visible radiation and excite these electrons to higher energy states i.e., the anti- bonding molecular orbitals. There are four such possible types of transitions. UV- Visible spectrophotometers are of two types' single beam and Dual beam spectrophotometers. Single beam spectrophotometers have only single cuvette but in the double beam there are two cuvettes. The minimum requirements of these spectrophotometers are source, monochromator, sample handling and detector. The sample handling is done with the help of cuvettes. Cuvettes are nothing but optically transparent cells hold the material under study and are used to introduce sample in to the light path. In order to eliminate the o source of error reference measurement is done in the cuvettes with same path length and not containing the

substance to be measured. In UV-Visible spectroscopy the standard cuvette containing the pure solvent does not absorb in the spectral region under consideration.

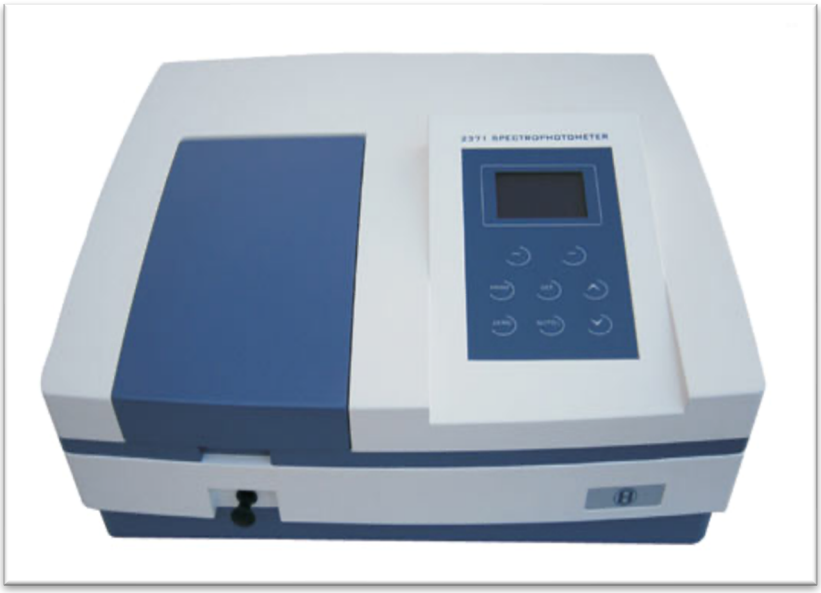

Figure: 2.3 UV spectrophotometer

UV-Visible spectra are also used for calculating band gap of semiconductor nanomaterials. In this a monochromatic light is passed through the sample and reference. After transmission they are reflected back in to the detectors where they compare the difference.

CHAPTER-3

RESULT AND DISCUSSION

3.1 Structural Analysis

The XRD patterns of all the materials of MgO pure and Co doped (1 %) elaborated by modified auto-combustion method are shown in Fig. 1. The spectra show crystalline materials with planes lying at (111), (200) and (220) for pristine MgO, and at (311) and (222) for Co doped sample [48]. All peaks are identical to those corresponding to the MgO phase indexed in the cubic phase magnesium oxide structure with an Fm-3 m space group, as described in the 45-0946 JCPDS card and the lattice parameters, a = b = c 4.2260 A˚, α=β=γ = 90° and lattice volume, V = 75.4717 Å^3, which are in good agreement with those observed in earlier studies [49]. The strong intensity of the peaks representing the preferential orientation in the (111), (200) and (220) planes indicates that the nanoparticles exhibit good crystallinity. The average crystallite size, D of the undoped and Co doped Mg0.99Co0.01O samples have been estimated from the X-ray spectra, using the following Scherrer's formula:

$$D = 0.9\lambda / \beta \cos\theta$$

where λ is the wavelength of Cu-K radiation (λ = 1.5405 Å), θ the diffraction angle and β the full width of the diffraction line measured at half of its maximum intensity, in radians.

where λ is the wavelength of Cu-K radiation (λ = 1.5405 Å), θ the diffraction angle and β the full width of the diffraction line measured at half of its maximum intensity, in radians.

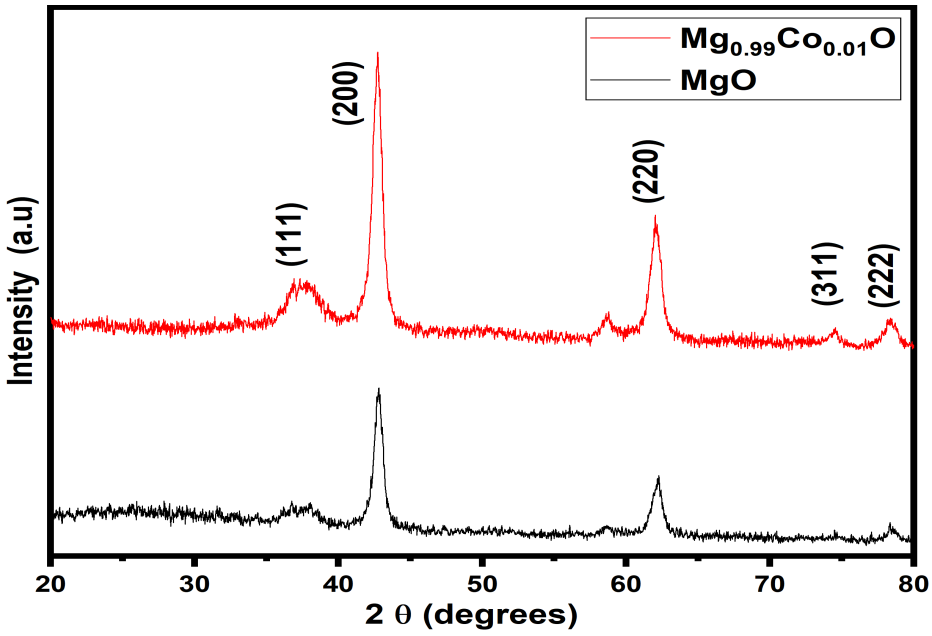

Fig.1 XRD pattern of MgOand$Mg_{0.99}Co_{0.01}O$ nanoparticle

As shown in the **Table 1**, the crystallite size of the nanoparticles is seen to increase with increase in Co concentration. This result can be justified by the enhanced incorporation of Co^{3+} ions into the Mg^{2+} sites of the host MgO lattice. This increase in crystallite size with the increase in Co concentration reflects an enhancement of the crystalline quality of the nanoparticles and consequently the decrease in grain boundary scattering [49].

Table.1. Crystallite size of pristine MgO and Co doped $Mg_{0.99}Co_{0.01}O$ nanoparticle

Sample code	Crystallite size –D (nm)
MgO	**21.04**
$Mg_{0.99}Co_{0.01}O$	**23.56**

3.2 Optical Analysis

Ultraviolet absorption is a process in which the outer electrons of atoms or molecules absorb radiant energy and undergo transitions to high energy levels. In this process, the spectrum obtained due to optical absorption can be analyzed to get the energy band gap of the material. MgO is reported to exhibit a broad absorption peak in between 260-330 nm [50].

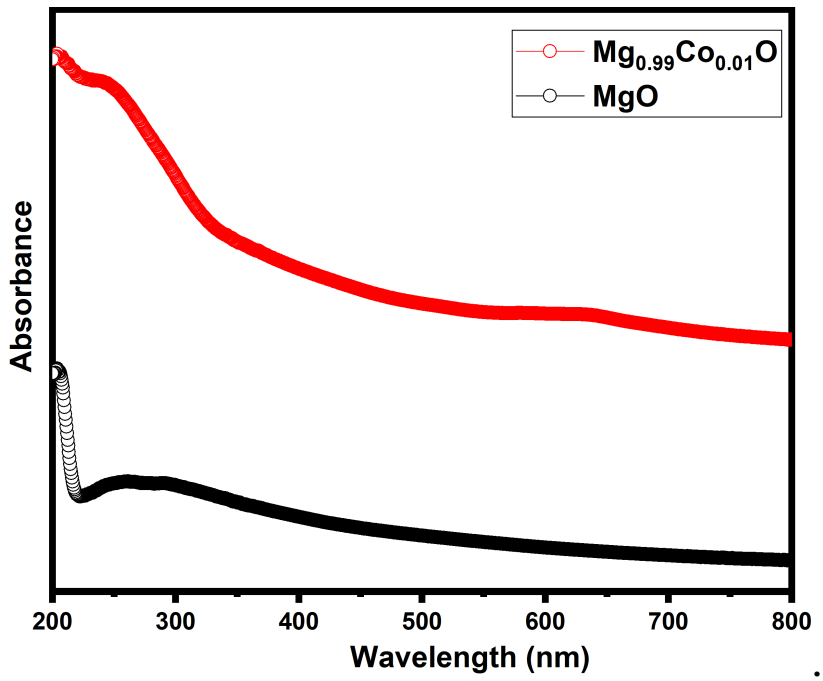

Fig.2 (a) UV-Visible absorbance spectrum of MgO and $Mg_{0.99}Co_{0.01}O$

Fig. 2 (a) shows the optical absorption spectrum of MgO and Co doped $Mg_{0.99}Co_{0.01}O$ nanostructures respectively. The spectrum shows the general trend of absorption i.e the absorbance of the material decreases with increase in wavelength of incident radiation.

In optical devices, band gap energy remains one of the main characteristics of the synthesized materials, which must be determined. The optical band gap energy of the materials have been determined by means of the Tauc's equation, which translates the relation between the absorption coefficient (α) and the incident energy (hν). This relation is given by the equation [51].

$$(\alpha h\nu)^2 = A(h\nu - Eg)$$

where A is constant and has different values for different transitions, hν is the photon energy and E_g is the optical band gap energy. The variation of $(\alpha h\nu)^2$ with photon energy (hν) for all synthesized nanostructures are shown in **Fig.3**

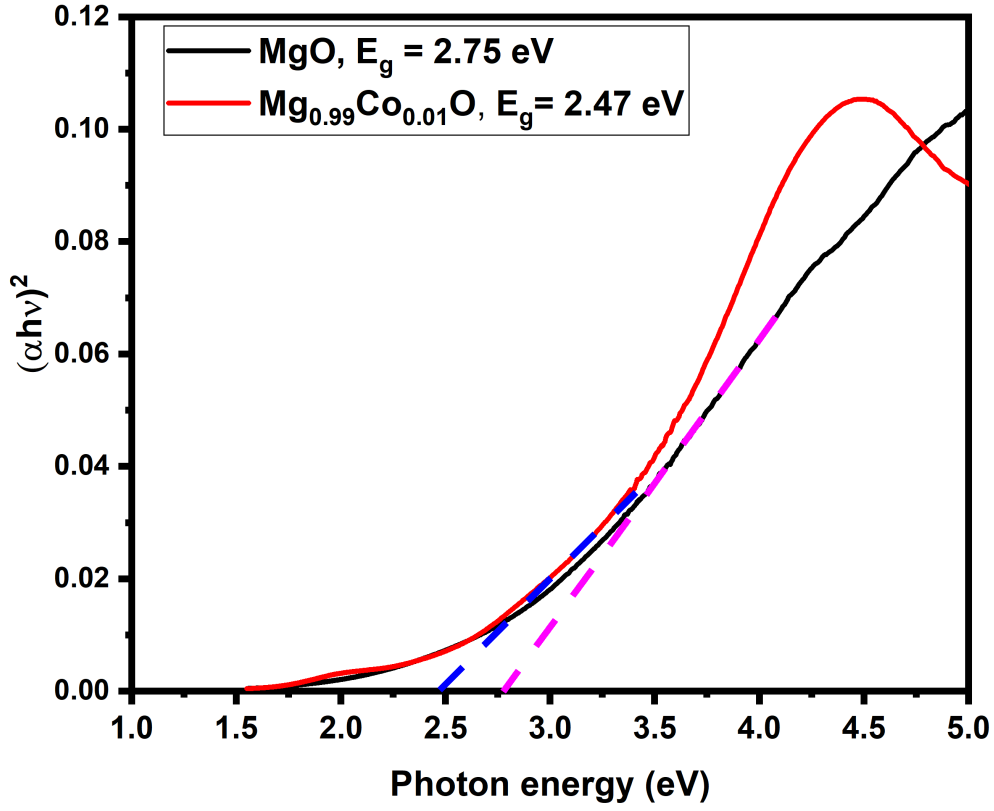

Fig.3 Bandgap of MgOand $Mg_{0.99}Co_{0.01}O$

The results obtained from the Tauc plot are grouped in **Table .2.** The value of the optical band gap energy (Eg) of the undoped sample is found to be equal to 2.75 eV, very close to reported values [52]. For the doped samples, optical energy band gap goes on decreasing to

2.47 eV with increasing Co content, which may be caused by the presence of surface defects or interstitial defects. Presence of such defects creates some intermediate energy levels between the valence band and the conduction band.

Table.2. Bandgap of MgO and $Mg_{0.99}Co_{0.01}O$

Sample code	**Bandgap (eV)**
Cr_2O_3	**2.75**
$Cr_{1.99}Co_{0.01}O_3$	**2.47**

CHAPTER – 4

CONCLUSION

Nanostructures of pristine and Co doped MgO have been synthesized using a modified auto-combustion method, which have been characterized with the aid of X-ray diffraction and UV-Visible spectroscopy. The XRD analysis of pure and Co doped MgO nanostructures show strong intensity peaks representing preferential orientation in the (111), (200) and (220) planes indicating that the nanoparticles exhibit good crystallinity. The average crystallite size of the undoped and Co doped samples have been determined to be 21.04 nm and 23.56 nm respectively. The increase in crystallite size with the increase in Co concentration reflects an enhancement of the crystalline quality of the nanoparticles and consequently the decrease in grain boundary scattering. The UV-Visible spectrum of the samples shows a general trend of absorption and the absorbance is seen to decrease with increase in the wavelength of incident radiation. Tauc plot analysis reveals the optical bandgap of pure MgO nanoparticles as 2.75 eV and that of Co doped sample as 2.47 eV.

REFERENCES

1. Cottrell, T. L. (1958). The Strengths of Chemical Bonds, Butterworths, London.
2. CrystalExplorer, V. (2012). 3.0, SK Wolff, DJ Grimwood, JJ McKinnon, MJ Turner, D. Jayatilaka, MA Spackman, University of Western Australia.
3. Cui, Y., Yue, Y., Qian, G., & Chen, B. (2012). Luminescent functional metal–organic frameworks. Chemical reviews, 112(2), 1126-1162.
4. El-Azhary, A. A., & Suter, H. U. (1996). Comparison between optimized geometries and vibrational frequencies calculated by the DFT methods. *The Journal of Physical Chemistry*, *100*(37), 15056-15063
5. Cullity, B. D. (1956). *Elements of X-ray Diffraction*. Addison-Wesley Publishing.
6. Debrus, S., Ratajczak, H., Venturini, J., Pincon, N., Baran, J., Barycki, J., ... & Pietraszko, A. (2002). Novel nonlinear optical crystals of noncentrosymmetric structure based on hydrogen bonds interactions between organic and inorganic molecules. Synthetic Metals, 127(1-3), 99-104.
7. Deepa, B., & Philominathan, P. (2016). Optical, mechanical and thermal behaviour of Guanidinium Carbonate single crystal. *Optik*, *127*(3), 1507-1510.
8. Y. Xia, P. Yang, Y. Sun, Y. Wu, B. Mayers, B. Gates (2003) One-dimensional nanostructures: synthesis, characterization and applications, 15(5),353-389.
9. Degiorgio, V., & Flytzanis, C. (Eds.). (1995). Nonlinear optical materials: principles and applications (Vol. 126). IOS Press.
10. Xinxiao Zhou, Bin Liu, Yun Chen, Lei Guo and Gang Wei (2020) Carbon nanofiber-based three-dimensional nanomaterials for energy and environmental applications, Qingdao University, 2163-2181.
11. Qiong Wu, Wei-shou Miao, Yi-du Zhang, Han-jun Gao and David Hui (2020) Mechanical properties of nanomaterials: A review, Nanotechnology Reviews,2020-0021.
12. Dan Guo, Guoxin Xie and Jianbin Luo (2013) Mechanical properties of nanoparticles:
    a. basics and applications, State Key Laboratory of Tribology, Department of Mechanical Engineering, Tsinghua University, Beijing 100084, People's Republic of China, 0022-3727.
13. Niranjan Karak (2019) Fundamentals of Nanomaterials and Polymer Nanocomposites.
14. Jun Tang (2014), Nanoparticles Self-assembly and application to chemical sensors, LAP
15. Atharvinamdar (2019) What are the methods used in nano Material synthesis Subject Expert, Datta Meghe College of Engineering.

16. Guozhong Cao., “Nanostructure and Nanomaterials Synthesis, properties and applications”.
17. Pan, J. S., & Zhang, X. W. (2006). Structure and dielectric behavior of Pb (Mg1/3Nb2/3) O3–Pb (Ni1/3Nb2/3) O3–Pb (Zn1/3Nb2/3) O3–PbTiO3 ferroelectric ceramics near the morphotropic phase boundary. Acta materialia, 54(5), 1343-1348.
18. Pandian, M. S., Boopathi, K., Ramasamy, P., & Bhagavannarayana, G. (2012). The growth of benzophenone crystals by Sankaranarayanan–Ramasamy (SR) method and slow evaporation solution technique (SEST): a comparative investigation. Materials Research Bulletin, 47(3), 826-835.
19. Yong X. Gan (2020) Hydrothermal Synthesis of Nanomaterials, Department of Mechanical Engineering, California State Polytechnic University Pomona, 3801 W. Temple Avenue, Pomona, CA 91768, USA
20. O'Donoghue, M. (1983). A guide to Man-made Gemstones. Great Britain: Van Nostrand Reinhold Company. pp. 40–44. ISBN 0-442-27253-7.
21. 21.Trotta, F.; Mele, A. Nanomaterials: Classification and Properties. In Nanosponges; John Wiley & Sons, Ltd.: Hoboken, NJ, USA,2019; pp. 142–149. ISBN 978-3-527-34100-9.
22. Hannah, W.; Thompson, P.B. Nanotechnology, Risk and the Environment: A Review. J. Environ. Monit. 2008, 10, 291–300.[CrossRef] [PubMed]
23. Jeevanandam, J.; Barhoum, A.; Chan, Y.S.; Dufresne, A.; Danquah, M.K. Review on Nanoparticles and Nanostructured Materials:History, Sources, Toxicity and Regulations. Beilstein J. Nanotechnol. 2018, 9, 1050–1074. [CrossRef] [PubMed]
24. Saleh, T.A. Nanomaterials: Classification, Properties, and Environmental Toxicities. Environ. Technol. Innov. 2020, 20, 101067.[CrossRef]
25. Malhotra, B.D.; Ali, M.A. Chapter 1-Nanomaterials in Biosensors: Fundamentals and Applications. In Nanomaterials for Biosensors;Malhotra, B.D., Ali, M.D.A., Eds.; Micro and Nano Technologies; William Andrew Publishing: Norwich, NY, USA, 2018; pp. 1–74. ISBN 978-0-323-44923-6.
26. Danish, M.S.S.; Bhattacharya, A.; Stepanova, D.; Mikhaylov, A.; Grilli, M.L.; Khosravy, M.; Senjyu, T. A Systematic Review of Metal Oxide Applications for Energy and Environmental Sustainability. Metals 2020, 10, 1604. [CrossRef]
27. Chavali, M.S.; Nikolova, M.P. Metal Oxide Nanoparticles and Their Applications in Nanotechnology. SN Appl. Sci. 2019, 1, 607.[CrossRef]

28. Duffy, T.; Madhusudhan, N.; Lee, K.K.M. 2.07-Mineralogy of Super-Earth Planets. In Treatise on Geophysics, 2nd ed.; Schubert, G.,Ed.; Elsevier: Oxford, UK, 2015; pp. 149–178. ISBN 978-0-444-53803-1. [CrossRef]
29. Cheremisinoff, N.P.V. Condensed Encyclopedia of Polymer Engineering Terms; Cheremisinoff, N.P., Ed.; Butterworth-Heinemann:Boston, MA, USA, 2001; pp. 340–347. ISBN 978-0-08-050282-3.
30. Akinwekomi, A.D.; Tang, C.-Y.; Tsui, G.C.-P.; Law, W.-C.; Chen, L.; Yang, X.-S.; Hamdi, M. Synthesis and Characterisation of Floatable Magnesium Alloy Syntactic Foams with Hybridised Cell Morphology. Mater. Des. 2018, 160, 591–600. [CrossRef]
31. Singh, J.P.; Chae, K.H. D° Ferromagnetism of Magnesium Oxide. Condens. Matter 2017, 2, 36. [CrossRef]
32. Collaboration: Authors and editors of the volumes III/17B-22A-41B Magnesium oxide (MgO) crystal structure, lattice parameters,thermal expansion. In II-VI and I-VII Compounds; Semimagnetic Compounds; Madelung, O., Rössler, U., Schulz, M., Eds.; Landolt-Börnstein-Group III Condensed Matter; Springer: Berlin/Heidelberg, Germany, 1999; Volume 41b, pp. 1–6. ISBN 978-3-540-64964-9. [CrossRef]
33. Green, J. Calcination of Precipitated Mg (OH)2 to Active MgO in the Production of Refractory and Chemical Grade MgO. J. Mater.Sci. 1983, 18, 637–651. [CrossRef]
34. Margarete Seeger; Walter Otto; Wilhelm Flick; Friedrich Bickelhaupt; Otto S. Akkerman. "Magnesium Compounds". Ullmann's Encyclopedia of Industrial Chemistry. Weinheim: Wiley-VCH.
35. V. Štengl, S. Bakardjieva, M. Maříková, P. Bezdička, and J. Šubrt, “Magnesium oxide nanoparticles prepared by ultrasound enhanced hydrolysis of Mg-alkoxides,” Materials Letters, vol. 57, no. 24-25, pp. 3998–4003, 2003.
36. M. B. Gawande, P. S. Branco, K. Parghi et al., “Synthesis and characterization of versatile MgO-ZrO2 mixed metal oxide nanoparticles and their applications,” Catalysis Science & Technology, vol. 1, no. 9, pp. 1653–1664, 2011.
37. Z. Camtakan, S. Erenturk, and S. Yusan, “Magnesium oxide nanoparticles: preparation, characterization, and uranium sorption properties,” Environmental Progress and Sustainable Energy, vol. 31, no. 4, pp. 536–543, 2012.
38. L.A. Ma, Z.X. Lin, J.Y. Lin, Y.A. Zhang, L.Q. Hu and T.L. Guo:Physica E 41 (2009), p. 1500-1503.
39. V. Kumar, M.K. Sharma, J.Gaur, T.P.Sharma: Letters 5 (2008), p. 289 – 295.

40. A.M.E. Raj, V.B. Jothy, C. Ravidhas, T. Som, M. Jayachandran,C. Sanjeeviraja: Radiation Physics and Chemistry 78 (2009), p. 914-921.
41. Mohammed M. Obeid, Shaker J. Edrees, Majid M. Shukur Synthesis and characterization of pure and cobalt dopedmagnesium oxide nanoparticles: Insight from experimental and theoretical investigation Superlattices and Microstructures (2018)
42. Jingjun Wu, Fangming Liu, Jiawei Zhang, Qiang Wang, Yinjuan Liu, Jin Liu, Ke Liu & Duanwei He (2018) Cobalt-doped magnesium oxide pressure-transmitting medium for high pressure and high-temperature apparatus, High Pressure Research, 38:4, 448-457,
43. Balakrishnan, G.; Velavan, R.; Mujasam Batoo, K.; Raslan, E.H. Microstructure, Optical and Photocatalytic Properties of MgO Nanoparticles. Results Phys. 2020, 16, 103013. [CrossRef] [PubMed]
44. Suresh, J.; Yuvakkumar, R.; Sundrarajan, M.; Hong, S.I. Green Synthesis of Magnesium Oxide Nanoparticles. Adv. Mater. Res. 2014, 952, 141–144. [CrossRef]
45. Devaraja, P.B.; Avadhani, D.N.; Prashantha, S.C.; Nagabhushana, H.; Sharma, S.C.; Nagabhushana, B.M.; Nagaswarupa, H.P. Synthesis, Structural and Luminescence Studies of Magnesium Oxide Nanopowder. Spectrochim. Acta Part Mol. Biomol. Spectrosc. 2014, 118, 847–851. [CrossRef]
46. Wahab, R.; Ansari, S.G.; Dar, M.A.; Kim, Y.S.; Shin, H.S. Synthesis of Magnesium Oxide Nanoparticles by Sol-Gel Process. Mater. Sci. Forum 2007, 558–559. 983–986. [CrossRef]
47. Barbara L Dutrow, X-ray Powder Diffraction (XRD) Instrumentation - How Does It Work?, Louisiana State University , Christine M. Clark, Eastern Michigan University.
48. Mirzaei, H., &Davoodnia, A. (2012). Microwave assisted sol-gel synthesis of MgO nanoparticles and their catalytic activity in the synthesis of hantzsch 1, 4-dihydropyridines. Chinese journal of catalysis, 33(9-10), 1502-1507.
49. Obeid, M. M., Edrees, S. J., &Shukur, M. M. (2018). Synthesis and characterization of pure and cobalt doped magnesium oxide nanoparticles: Insight from experimental and theoretical investigation. Superlattices and Microstructures, 122, 124-139.
50. Almontasser, A., Parveen, A., &Azam, A. (2019, November). Synthesis, Characterization and antibacterial activity of Magnesium Oxide (MgO) nanoparticles. In IOP Conference Series: Materials Science and Engineering (Vol. 577, No. 1, p. 012051). IOP Publishing.
51. Alajerami, Y. S. M., Hashim, S., Ghoshal, S. K., Ramli, A. T., Saleh, M. A., Ibrahim, Z., Bradley, D. A. (2013). Luminescence characteristics of Li2CO3–K2CO3–H3BO3 glasses co-doped with TiO2/MgO. Applied Radiation and Isotopes, 82, 12-19.

52. Bindhu, M. R., Umadevi, M., Micheal, M. K., Arasu, M. V., & Al-Dhabi, N. A. (2016). Structural, morphological and optical properties of MgO nanoparticles for antibacterial applications. Materials Letters, 166, 19-22